Journal of Physics: Conference Series **485** (2014) 012052 doi:10.1088/1742-6596/485/1/012052

DisCERNing new physics in $t\bar{t}$-production from top-spin observables

Blaženka Melić

Rudjer Bošković Institute, Theoretical Physics Division, Bijenička 54, HR-10000 Zagreb, Croatia

E-mail: melic@thphys.irb.hr

Abstract. We examine the models of new physics which could potentially explain the significant deviation of the measured forward-backward asymmetry in $t\bar{t}$ production at the Tevatron from the SM prediction, by fitting the models to the all available $t\bar{t}$ production data. To be able further to discriminate among the NP models we calculate predictions for various top spin polarization and top-antitop spin correlation observables at Tevatron and the LHC.

1. Introduction

The top quark physics is interesting due to the several reasons. Top quark is the heaviest of the quarks with a mass comparable with the electroweak symmetry breaking (EWSB) scale. Due to its heaviness it decays very fast and it does not hadronize. Moreover, its coupling to the Higgs is of $O(1)$, and therefore the understanding of the top quark properties provides the insight into the nature of the EWSB mechanism.

Hadron collider experiments at Tevatron and LHC have greatly enriched our knowledge about the top quark physics measuring precisely the $t\bar{t}$ production cross section and its invariant mass ($m_{t\bar{t}}$) production, forward-backward (A_{FB}) or charge asymmetries (A_C) in the production, as well as the single top production with already impressive precision. While other top properties exhibit an agreement with the Standard model predictions, the D0 and CDF experiments are constantly observing anomalously large A_{FB} at $\geq 2\sigma$ level (c.f. [1] for a recent review).

In order to explain these puzzling phenomena at Tevatron, there were several New Physics (NP) models proposed, interfering with the SM contribution by exchange of the new s, t or u-channel resonances. To distinguish among the models, it is important to investigate all possible observables, such as the shape of $A_{FB}(m_{t\bar{t}})$, the resonant peaks in $\sigma_{t\bar{t}}(m_{t\bar{t}})$ or the top quark spin polarization and spin correlations, being the subject of this work [2].

2. Asymmetries and the NP models

Asymmetries in the $t\bar{t}$ production are defined differently for the Tevatron and for the LHC machine. At the Tevatron the A_{FB} is taken as the asymmetry between the production rates in the forward and the backward region, while at the LHC, since it is a symmetric pp machine, there is is no preferred global direction and $A_{FB} = 0$. However, there it is possible to define the charge asymmetry, A_C, since the tops are more forward than antitops (because inside the proton the valence quarks are more boosted than the sea antiquarks). Therefore there is an excess of

boosted top quarks along the beam axis and $A_C \neq 0$. For theories with the CP-conserving couplings $A_{FB} = A_C$.

In the SM the asymmetries arise at NLO, and are robust under high-energy QCD corrections [3], while the electroweak corrections contribute to 20% [4]. The SM predicts a small, but non-zero asymmetry in the $t\bar{t}$ production, being $A_{FB}^{SM} \sim 7 - 9\%$ and $A_C^{SM} \sim 1\%$. While the LHC measurements give $A_C = 0.001 \pm 0.0014$, consistent with the SM prediction, the D0 and CDF are consistently observing anomalously large forward-backward asymmetries:

$$\begin{aligned} A_{FB} &= 0.187 \pm 0.037\,, \\ A_{FB}^{low} &\equiv A_{FB}(m_{t\bar{t}} < 450\ \text{GeV}) = 0.078 \pm 0.054\,, \\ A_{FB}^{high} &\equiv A_{FB}(m_{t\bar{t}} > 450\ \text{GeV}) = 0.296 \pm 0.067\,, \end{aligned}$$

which have to be compared with $A_{FB}^{\rm SM} = 0.066(20)$ and $A_{FB}^{low,\rm SM} \simeq 0.047, A_{FB}^{high,\rm SM} \simeq 0.100$ [3].

To explain these deviations we consider several NP models, which generate asymmetry from the interference with the SM by exchanging new particles in s-channel (G'), t-channel (W', Z', ϕ (the neutral component of the isodublet Φ)), or u-channel (Δ, Σ). In the table 1 we summarize the NP models, together with their lagrangians and couplings considered in the fits. For all details consult [2].

Table 1. New physics models considered.

model	Lagrangian of interaction	fitted coupl.
s-channel: axigluon	$\mathcal{L}^{\rm int.}_{G'} = -\bar{q}(g_V^q - g_A^q\gamma_5)\not{G}' q - \bar{t}(g_V^t - g_A^t\gamma_5)\not{G}' t$	g_A^q, g_A^t
t-channel: Z'	$\mathcal{L}^{\rm int.}_{Z'} = -\bar{u}\gamma_\mu(f_L^{Z'}P_L + f_R^{Z'}P_R)tZ'$	$f_R^{Z'}$
W'	$\mathcal{L}^{\rm int.}_{W'} = -\bar{d}\gamma_\mu(f_L^{W'}P_L + f_R^{W'}P_R)tZ'$	$f_R^{W'}$
scalar doublet Φ	$\mathcal{L}^{\rm int.}_{\Phi} = -y^u_{ij}\bar{q}_{Li}u_{Rj}\Phi - y^d_{ij}\bar{q}_{Li}d_{Rj}\tilde{\Phi}$	y^u_{ij}
u-channel: scalar color triplet Δ	$\mathcal{L}^{\rm int.}_{\Delta} = -g_{(\Delta)ij}\epsilon_{abc}\bar{u}^a_{R,i}(u^b_{R,j})^C\Delta^C$	$g_{(\Delta)ij}$
scalar color sextet Σ	$\mathcal{L}^{\rm int.}_{\Sigma} = -g_{(\Sigma)ij}\ (\bar{u}^a_{R,i}(u^b_{R,j})^C + \bar{u}^b_{R,i}(u^a_{R,j})^C)\Sigma^{ab\dagger}$	$g_{(\Sigma)ij}$

3. New physics model selections

New models must explain large asymmetries without significantly changing the cross-section predictions, which are already measured at 7% precision and are in agreement with the SM calculations [5]. To select the models we perform two fits to the available data. One, scenario A, is a global χ^2 fit to the following observables $A = \{A_{FB}, A_C, \sigma_{Tev}, \sigma_{Tev}^{high}, \sigma_{LHC}\}$, while in the scenario B we use the data on $\{A_{FB}^{low}, A_{FB}^{high}, d\sigma_{Tev}/dm_{t\bar{t}}, \sigma_{LHC}\}$ in the fit. We consider NP model as acceptable if it improves upon SM χ^2 ($\chi^2_{A,\rm SM} = 2.3$/d.o.f. in approach A and $\chi^2_{B,\rm SM} = 1.8$/d.o.f. in approach B). The results of the fits are shown in figures 1-4.

For the axigluon model, in the approach B, our model fit selects two parameter regions shown in figure 1: low axigluon mass region with $m'_G < 450$ GeV and $g_A^u g_A^t \sim 0.2$ and the high mass region with $m'_G > 700$ GeV and $g_A^u g_A^t \sim -0.5$.

For the Z' and W' models, we see from the figures 2 that the A_{FB} and A_C measurements are highly correlated and that the tension between them cannot be reduced below 2σ level, and therefore we exclude these NP models from the further consideration.

The neutral field ϕ of the scalar isodoublet model exhibits two allowed parameter regions: the more preferred low m_ϕ mass region, $m_\phi < m_t$ in the approach A, and $m_\phi > 200$ GeV in the scenario B, figure 3.

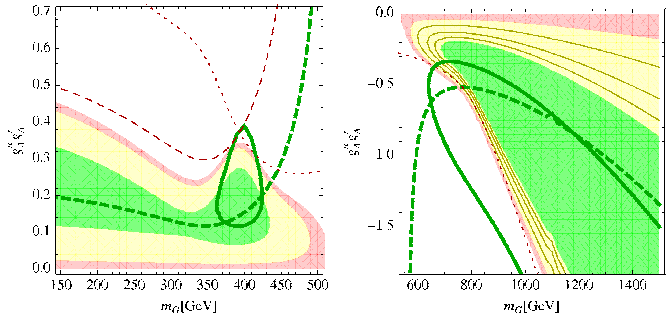

Figure 1. $t\bar{t}$ production constraints on *the axigluon model* in the low (left plot) and high (right plot) mass region in the approach B: binned A_{FB} at 1σ in thick full green line, inclusive A_C at 1σ (2σ) in thick dashed green line (thin dashed red line), $m_{t\bar{t}}$ spectrum at 2σ in thin red dotted line. Parameter regions where the model can improve the SM χ^2 by $-\Delta\chi^2 > 0, 1, 4$ are shaded in red, yellow and green respectively.

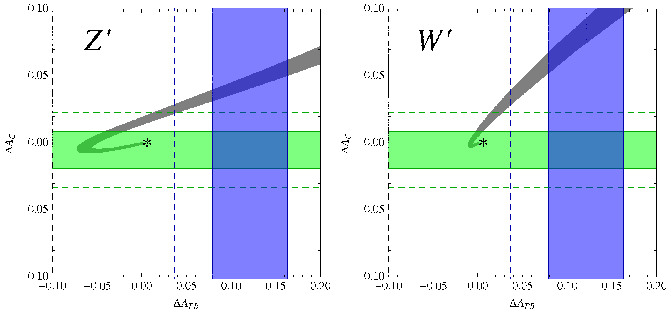

Figure 2. Correlation between the $\Delta A_{FB} = A_{FB} - A_{FB}^{SM}$ and $\Delta A_C = A_C - A_C^{SM}$ contributions of Z' (left plot) and W' (right plot) *models* in shaded narrow gray bands using the approach A. The thickness of the bands is given by the Z' (W') mass variation in the range $[100, 500]$ GeV. The Tevatron average of ΔA_{FB} at 1σ (2σ) is represented by the vertical blue band (dashed vertical lines). The ATLAS measurement of ΔA_C (the SM reference point is marked with "*") at 1σ (2σ) is represented by the horizontal green band (dashed horizontal lines). The tension between the two observables increases with increasing mediator mass (inner edge of the band corresponds to lowest mediator mass).

As for the NP models in the u-channel exchange of new particle, there are some tensions between A_{FB} and the $t\bar{t}$ spectrum measurements, in particular at high $m_{t\bar{t}}$ region, figure 4. However, taking into account the possible caveats of the $d\sigma/dm_{t\bar{t}}$ constraints, we retain the Δ and Σ model parameter regions preferred in the approach A in our analysis of top spin observables.

4. Top spin polarization and spin correlations

Due to the different production mechanisms of top-antitop pairs at Tevatron and LHC, there is a difference in the produced asymmetries. The Tevatron produces about 90% of $t\bar{t}$ pairs in the $q\bar{q}$-annihilation, and just 10% pairs come from the gg-fusion. For the LHC, which is a symmetric proton-proton machine, the situation is just opposite. Furthermore, depending on the production mechanism top quarks are produced in a definite spin configurations. At the threshold, in $q\bar{q}$-annihilation, the produced tops are in $t_L\bar{t}_R$ or $t_R\bar{t}_L$ configuration, while the produced top-antitop pairs from gluons come out in LL and RR spin configuration. Since the top decays before it

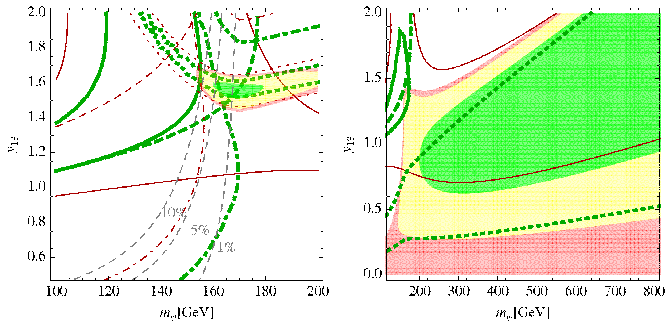

Figure 3. $t\bar{t}$ production constraints on *the scalar isodoublet model* in approach A (left plot) and B (right plot): FBA (inclusive in left plot and binned in right plot) at 1σ (2σ) in thick full green line (thin full red line), inclusive CA at 1σ (2σ) in thick dashed green line (thin dashed red line). In left plot $\sigma_{\rm TEV}$ at 1σ (2σ) in thick green dotted line (thin red dotted line), $\sigma_{\rm LHC}$ at 1σ (2σ) in thick green dash-dotted line (thin red dash-dotted line). In right plot $m_{t\bar{t}}$ spectrum at 1σ (2σ) in thick green dotted line (thin red dotted line). Parameter regions where the model can improve the SM χ^2 by $-\Delta\chi^2 > 0, 1, 4$ are shaded in red, yellow and green respectively. Finally in right plot for $m_\phi < m_t$, the contours of constant branching fraction $\mathrm{Br}(t \to u\phi^0)$ are displayed in thin gray dashed lines.

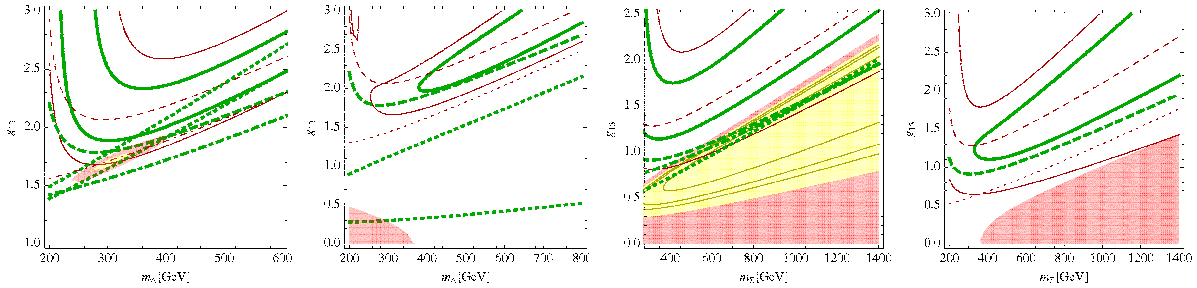

Figure 4. $t\bar{t}$ production constraints on *the scalar color triplet model* and *the scalar color sextet model* in approach A (left plot) and B (right plot): FBA (inclusive in left plot and binned in right plot) at 1σ (2σ) in thick full green line (thin full red line), inclusive CA at 1σ (2σ) in thick dashed green line (thin dashed red line). In left plot $\sigma_{\rm TEV}$ at 1σ (2σ) in thick green dotted line (thin red dotted line), $\sigma^h_{\rm TEV}$ at 2σ in thin red dash-dotted line. In right plot $m_{t\bar{t}}$ spectrum at 1σ (2σ) in thick green dotted line (thin red dotted line). Parameter regions where the model can improve the SM χ^2 by $-\Delta\chi^2 > 0, 1$ are shaded in red and yellow respectively.

hadronizes, almost exclusively in W^+b, the decay products contain information about the top spin. The top events are classified according to the W-decay products as dileptonic (with the branching ratio (BR) of $O(5\%)$ and a low background), leptonic + jets (with BR $\sim O(30\%)$ and a moderate background) and a purely hadronic events, with the largest BR $\sim O(46\%)$, but also a huge (QCD) background. By measuring the angular distributions of the decay products, we can determine the top polarization and top-antitop spin correlations [6] using the double differential angular distribution:

$$\frac{1}{\sigma}\frac{d^2\sigma}{d\cos\theta_f d\cos\theta_{\bar{f}}} = \frac{1}{4}\left(1 + \kappa_f B_t \cos\theta_f + \kappa_{\bar{f}} B_{\bar{t}} \cos\theta_{\bar{f}} - \kappa_f \kappa_{\bar{f}} C \cos\theta_f \cos\theta_{\bar{f}}\right) , \qquad (1)$$

where $\theta_f(\theta_{\bar{f}})$ is the angle between the direction of the top (antitop) spin analyzer f, $(\bar{f})$ (which can be either a direct t $(\bar{t})$ daughter W^+, b $(W^-, \bar{b})$ or a $W^+(W^-)$ decay product $\ell^+(\ell^-), \nu(\bar{\nu})$ or

jets) in the t ($\bar{t}$) rest frame. The top (antitop) spin analayzing power factors $\kappa_{f(\bar{f})}$, are different for the different top decaying products, being the largest for the leptons, $\kappa_{l^+(l^-)} = 1$, considered in this work. The coefficients $B_{t(\bar{t})}$ and C are connected with the spin observables $\langle\mathcal{O}\rangle_i$ as

$$\begin{aligned}
\mathcal{O}_1 &= \mathbf{S}_t \cdot \mathbf{S}_{\bar{t}} && \to \langle\bar{\mathcal{O}}_1\rangle = D\,, \\
\mathcal{O}_2 &= \mathbf{S}_t \cdot \hat{\mathbf{a}}\,, \quad \bar{\mathcal{O}}_2 = \mathbf{S}_{\bar{t}} \cdot \hat{\mathbf{b}} && \to \langle\mathcal{O}_2\rangle = B_t \quad \text{and} \quad \langle\bar{\mathcal{O}}_2\rangle = B_{\bar{t}}\,, \\
\mathcal{O}_3 &= 4(\mathbf{S}_t \cdot \hat{\mathbf{a}})(\mathbf{S}_{\bar{t}} \cdot \hat{\mathbf{b}}) && \to \langle\mathcal{O}_3\rangle = C\,.
\end{aligned} \tag{2}$$

and give the net spin polarization of the top-antitop system, polarization of the (anti) top quark, and the top-antitop spin correlation, both with respect to spin quantization axes $\hat{\mathbf{a}}$ and $\hat{\mathbf{b}}$, respectively, and D is measured in the opening angle distribution

$$\frac{1}{\sigma}\frac{d\sigma}{d\cos\phi} = \frac{1}{2}\left(1 - D\cos\phi_{f\bar{f}}\right)\,, \tag{3}$$

where ϕ is the angle between the direction of flight of the two (top and antitop) spin analyzers, defined in the t and $\bar{t}$ frames, respectively. The spin quantization axes $\hat{\mathbf{a}}$ and $\hat{\mathbf{b}}$ can be chosen to maximize (or minimize) the desired polarization and correlation effects. We have been working with the following choices: $\hat{\mathbf{a}} = -\hat{\mathbf{b}} = \hat{\mathbf{k}}_1$ (helicity basis), $\hat{\mathbf{a}} = \hat{\mathbf{b}} = \hat{\mathbf{p}}$ (beamline basis), and $\hat{\mathbf{a}} = \hat{\mathbf{b}} = \hat{\mathbf{d}}_X$ (off-diagonal basis, specific for model X, which gives almost 100% correlations at Tevatron [7]), where $\hat{\mathbf{p}}$ is the direction of the incoming beam and $\hat{\mathbf{k}}_1$ is the direction of the outgoing top quark, both in the $t\bar{t}$ center of mass frame. The measurements of the spin correlation coefficients C are performed at D0 for the beam and the helicity axis, at the CDF for the off-diagonal axis and at the LHC for the helicity axis, and the good agreement with the SM calculation [6] is confirmed.

5. Results and conclusions

The predictions for the top spin observables at Tevatron and the LHC are shown in figure 5. For the Tevatron, the prediction for the off-diagonal axis are similar to the prediction for the beamline axis. We can see that the beamline axis has a potential to discriminate between the sextet on one side and the the scalar doublet and color triplet model, on the other side. By measuring the top spin along the helicity axis, B_{hel}, on can discriminate between the doublet Φ and the color triplet Δ models. As for the axigluon, to get some information, the precision of $O(2\%)$ is needed. At the LHC, although the helicity axis has a potential to discriminate between the scalar doublet and the axigluon models, generally, the axigluon model would be difficult to probe with the top spin observables. However, at the LHC, the measurement of the spin observables D, C_{beam} and B_{hel} at $O(5\%)$ could help to discern among the scalar models.

To conclude, among the considered models only an axigluon can reproduce all Tevatron observables, without being in severe tension with the recent LHC results on $t\bar{t}$ production cross section, charge asymmetry and top-spin correlations. The models with W' and Z' bosons are excluded as a possible explanation for the Tevatron A_{FB} anomaly by the LHC charge asymmetry measurements. We have demonstrated that future precise measurements of various top spin correlations and especially the top spin polarization could provide a significant constraints on possible explanations of the Tevatron A_{FB} anomaly, in particular in the scalar model channels.

Acknowledgments

The fruitful collaboration with J. Kamenik and S. Fajfer is acknowledged. I would also like to thank the organizers of the PASCOS2012 conference. The work is supported by the Ministry of Education, Science and Sport of the Republic of Croatia under contract No. 098-0982930-2864.

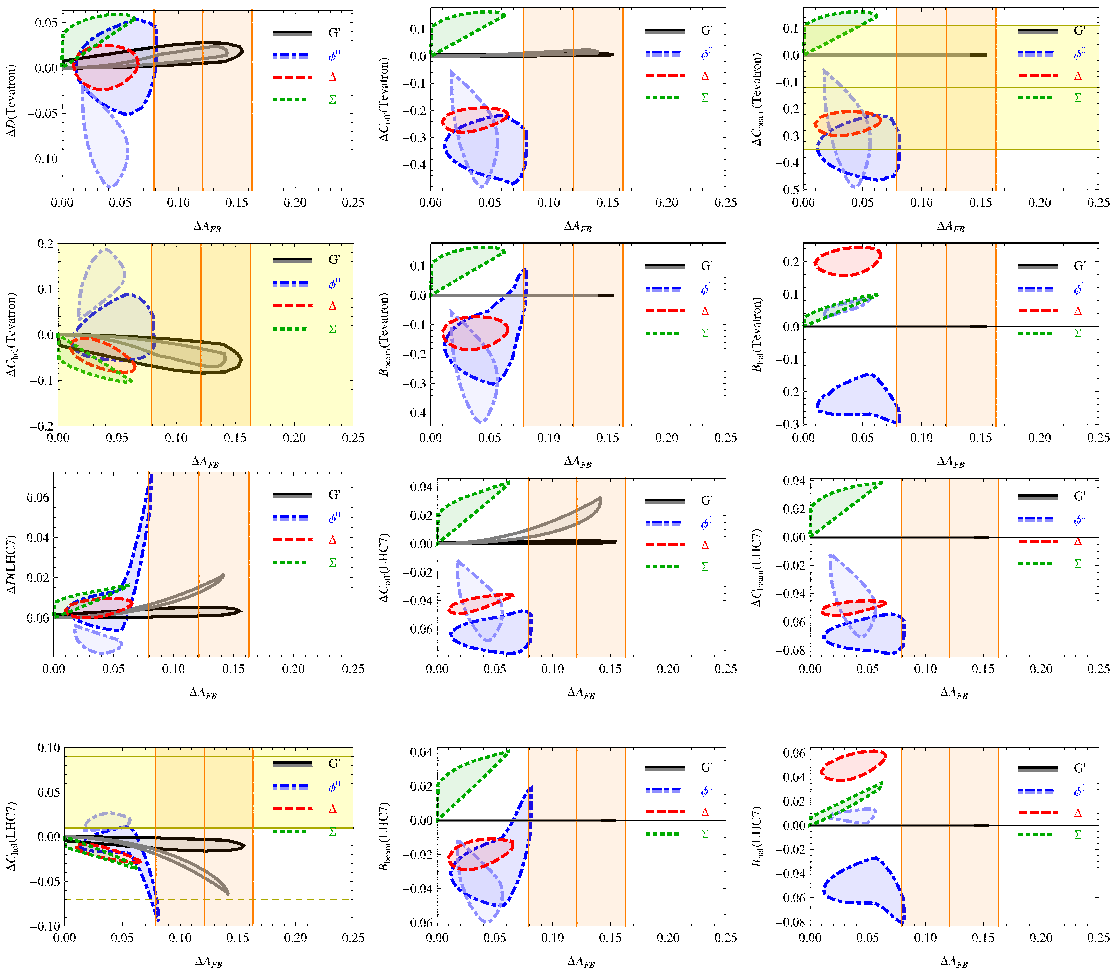

Figure 5. Correlations between the NP contributions to the inclusive A_{FB} and various spin observables at the Tevatron and at the 7 TeV LHC. The present experimental results (68% C.L. regions) are shaded in horizontal and vertical bands. The NP model predictions are determined from the global fit as specified in the text and are bounded by full (axigluon G' in the low ($m_G \lesssim 450$ GeV in black) and high ($m_G \gtrsim 700$ GeV in gray) mass regions), dashed (scalar color triplet Δ), dotted (scalar color sextet Σ) and dot-dashed (neutral component of the scalar isodoublet ϕ^0 in the low ($m_\phi \lesssim m_t$ in darker shade) and high ($m_\phi > 200$ GeV in lighter shade) mass region) contours. For $\Delta C_{\rm hel}$(LHC7) we also show the 95% C.L. contour in thin dashed line.

References

[1] Kamenik J F, Shu J and Zupan J Review of new physics effects in t-tbar production *Preprint* arXiv:1107.5257
[2] Fajfer S, Kamenik J F and Melić B 2012 *JHEP* **8** 114
[3] Ahrens V, Ferroglia A, Neubert M, Pecjak B D and Yang L L 2011 *Phys. Rev.* D **84** 074004
[4] Hollik W and Pagani D 2011 *Phys. Rev.* D **84** 093003
[5] Aguilar-Saavedra J A and Perez-Victoria M 2011 *JHEP* **1105** 034
Aguilar-Saavedra J A and Perez-Victoria M 2011 *Phys. Rev.* D **84** 115013
[6] Bernreuther W, Brandenburg A, Si Z G and Uwer P 2004 *Nucl. Phys.* B **690** 81
[7] Parke S J and Shadmi Y 1996 *Phys. Lett.* B **387** 199
Uwer P 2005 *Phys. Lett.* B **609** 271